Meso- FE simulation of progressive damage in textile composites using mesh superposition method

S.A. Tabatabaei[1,2], E. Bedogni[3] , A. R. Melro[4], D. Ivanov[4], S.V. Lomov[1,2]

[1] Department of Materials Engineering, KU Leuven, Kasteelpark Arenberg 44, B-3001 Leuven, Belgium, Emails: seyedahmad.tabatabaei@mtm.kuleuven.be; stepan.lomov@mtm.kuleuven.be
[2]SIM Program M3Strength, Technologiepark Zwijnaarde 935, Zwijnaarde B-9052, Belgium.
[3]Dipartimento di Ingegneria Industriale, Università di Parma, Parco Area delle Scienze 181/A, 43124 Parma, Italy, Email: enricobedogni@gmail.com
[4]Advanced Composites Centre for Science and Innovation (ACCIS), University of Bristol, Queen's Building, University Walk, Bristol, BS8 1TR, UK, Emails: antoni.melro@bristol.ac.uk, Dmitry.Ivanov@bristol.ac.uk

Keywords: Finite element simulation, Damage, Mesh superposition method, Textile composite.

Abstract
The paper investigates feasibility of application of mesh superposition method (MSP) to damage modeling of textile composites on an example of a woven laminate. The geometrical model of yarns is created using WiseTex software. The yarns and matrix meshes are superimposed using embedded element technique. Damage initiation and development under tensile loading and the resulting stress-strain curves are simulated using continuous damage mechanics approach based on Puck damage criterion and Zinoviev-type damage variables. There was a good agreemenet between the FE simulations and experimental results.

1. INTRODUCTION

Meso-scale finite element (FE) modeling is key to numerical simulation of textile composites in linear and non-linear material behavior. These include stiffness, strength and damage properties, for example. The prevailing method in meso-FE modeling of composite is the "full" or continuum mesh method [1-3]. In this approach, the volume continuity of the reinforcement and matrix are preserved. To do so, the Boolean operation is applied to the matrix volume while unit cell modeling. However, difficulties with quality meshing of the matrix volume near the matrix/ reinforcement interface and surface penetrations are the main drawback of the continuum mesh method in meso-FE modeling of textile composites [1-3]. A further modeling technique, the mesh superposition method (MSP) or non-continuum mesh method presents a radical solution of the meshing problems in FE models of heterogeneous materials. In the MSP method, the reinforcement mesh is placed inside the matrix mesh and a ''coupling equation'' is created to define a relation between the degrees of freedom of the two meshes [4]. The embedded elements called also "superimposed meshes"; were developed by Ortiz et al. [5] to enhance the performance of isoparametric elements in numerical modelling of localized deformations. The strain localization refers to a condition when the deformation concentrates in a band, namely the "shear band" due to the constitutive behaviour of the material. There is strain discontinuity in the boundary elements of shear band crossing the isoparametric elements [5]. To simulate the localized shear band problem numerically, Oritz et al. [5] extended the element interpolation by adding proper shape functions. Therefore, the added shape functions created a "non-conforming" element that did not satisfy the C° continuity across the element boundary [6]. To eliminate the extra DOF's the static condensation [7] method was implemented. However, the proposed method for shear band localization modelling was limited to "small displacement" gradient theory and "rate-independent" material behaviour. Belytschko and Fish [8-9] developed Oritz's shear band concept incorporating the strain fields both in the localized region and rest of elements. The

Excerpt from ISBN 978-3-00-053387-7

difference with Oritz's method was that the strain fields were considered as a localization band rather than a strain discontinuity.
Fish and Belytschko [9] extended the shear band approach for large deformation problems. They developed consistent relations for nodal force and stiffness matrix of localized elements. In the following, Fish introduced the "s-version" of finite element method [10] to resolve the structure of functions with high gradients such as crack propagation in solids and shocks in fluid mechanics since the uniform meshes in such regions need enormous amounts of elements and the computational cost is high [10]. Zako et.al [11-12] proposed a "M^3" (M-cube) method based on the superposition technique for multi-scale modelling of a plain weave [11] and a stitched fabric composites[12]. They discretized the domain of analysis into three different scales: micro, meso, and macro. Each scale is meshed separately; the full finite element stiffness matrix is created as superposition of the stiffness matrices for the different scales. Kurashiki et.al [13], Honda et.al [14], Ohyama, and et.al [15] advanced the M-cube method to damage modelling of woven, non-crimp and braided composites.
Jiang [16] proposed the "domain superposition technique (DST)" for woven composites modelling. In the DST the reinforcement parts and matrix are meshed separately and then superimposed by applying coupling equations to produce a combined model. The results of DST were compared with the full model for a plain weave composite with satisfactory results for stiffness and stress pattern even with rough meshes for DST. However, the full homogenised stiffness matrix of the composite was not investigated, the comparison of the local stress fields was carried on only superficially and other textile structures were not studied. Iarve et al. [17-18] proposed the independent mesh method (IMM) to model the complex geometries in the composites using the combination of direct and voxel-based meshes. In this method the tows and matrix were meshed independently and then superimposed to each other without requiring the conventional 3D meshing. To eliminate the volume redundancy the shape functions in the redundant regions were disregarded.
In the present work, to investigate the application of the MSP method in damage modelling of textile composites, 2D plain weave E-glass composite detailed studied experimentally [19-20] was used as a benchmark. The aim is to implement the well-known and accurate damage algorithms for simulation of intra-yarn crack initiation and propagation as well as matrix material degradation in the meso-scale. The composite was modeled in WiseTex [21-22] based on geometrical description and transformed into a finite element model for stiffness and damage calculations. The numerical simulations under different loading directions such as warp/weft and bias direction were compared with the experimental results [19-20].

2. MODEL DESCRIPTION

A single ply of a 2D plain weave glass/epoxy composite is initially created in WiseTex [21-22] based on the geometrical information provided in [19-20]. The modelled yarn volumes are imported to ABAQUS using a Python script. The single ply is stacked up with [0/90/90/0] sequences to build up a multi-layer configuration (see Figure 1). A unit cell volume with flat faces is created by cutting off the "excess" parts of the yarns; the overall fibre volume fraction in the composite is preserved. The unit cell dimension is 12.5×10.26×2.45 (mm) with the strength properties for the matrix and yarns given in Table 1 [23]. The intra-yarn and overall fibre volume fractions were 75% and 52% respectively. The homogenised elastic properties of the yarn material are E_1 = 54.4 GPa, $E_2 = E_3$ = 14.7 GPa, $v_{12} = v_{13}$ = 0.255, v_{23} = 0.422, $G_{12} = G_{13}$= 5.91 GPa, G_{23} = 5.18 GPa (axis *1* corresponds to the local yarn axis direction) and for the matrix material E = 2.9 GPa and v = 0.35.
The matrix box is modelled and superimposed with the yarns using the "embedded element (EE)" constraint to relate the spatial DOF's of the yarns and matrix. Both of the host and guest parts are meshed separately with 8-node hexahedral, reduced integration elements (see Figure 1). The average aspect ratio of elements in yarns and matrix was 1.83 and 1.01, respectively. In addition, to investigate the mesh sensitivity in damage simulations, three different configurations: rough, fine and the finest meshes are considered. For each structure, the number of elements across the middle yarn - shown with an arrow in Figure 2 - is 4, 11 and 18 respectively.

Excerpt from ISBN 978-3-00-053387-7

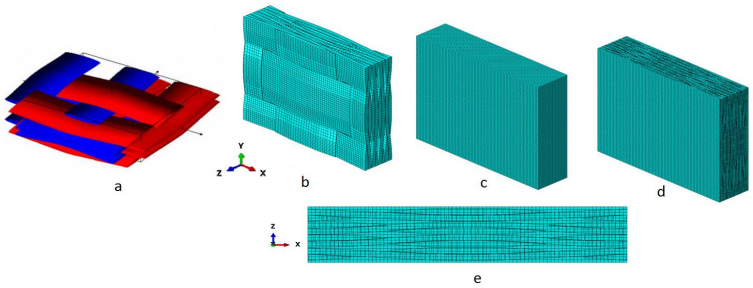

Figure 1. Unit cell model of plain weave composite in (a): WiseTex and (b)-(e) ABAQUS with the concept of embedded element method; (b) Yarns, (c) Matrix, (d) Superimposed yarns and matrix, (e) Side view of the unit cell.

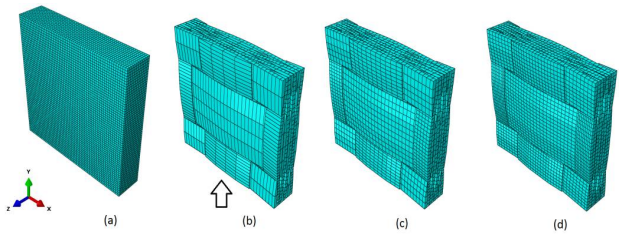

Figure 2. Mesh configurations in the multi-layer 2D plain weave glass/epoxy fabric used in damage analysis with MSP concept: (a) meshed matrix, (b), (c) , (d) rough , fine and the fines meshes in the yarns.

Table 1. Strength properties of yarns and matrix used in damage modelling [26].

Strength properties (MPa)	**Impregnated yarns**
Longitudinal tensile strength	1725
Longitudinal compressive strength	620
Transverse tensile strength	40
Transverse compressive strength	130
Shear strength	70
Strength properties (MPa)	**Matrix**
Tensile strength	76
Compressive strength	118
Shear strength	88

The idea of “contact algorithm” is implemented to cope with the yarn interpenetration in unit cell modelling of textile composite [2]. To eliminate the interpenetration, “penalty” formulation with friction coefficient of $1 \cdot 10^{-5}$ in tangential direction and “hard contact” method with “penalty” constraint in normal direction was applied between the surfaces of the impregnated yarns. The volume redundancy in the unit cell created by the mesh superposition was resolved using the “stiffness correction” approach in the redundant region proposed in [2]. The periodic boundary conditions [1] are applied to the faces of the unit cell during warp/weft and 45° loadings considering the Poisson’s effect in transverse to the loading directions. The unit cells are loaded to the failure strain of the individual glass fibre that is coincident with the fabric failure in the experiments.

Excerpt from ISBN 978-3-00-053387-7

3. DAMAGE ALGORITHM

The numerical simulation of progressive damage in the yarns that is based on experimental information in the meso- scale is incorporated into the mesh superposition method. A pressure dependent, elasto-plastic thermodynamically consistent damage model is implemented for matrix damage simulations [24]. The intra-yarn crack initiation and propagation is modelled using continuous damage mechanics (CDM) [25]. The CDM describes progressive stiffness degradation of rate-independent materials during tensile loading. Based on Ivanov damage model [26] the yarn is divided into small UD segments along the middle-line. In this way, the damage mechanics of a flat ply lamina can be implemented in each UD segment of the yarn [26]. The stress exposure factor (SEF) is evaluated in each UD fragment of the yarn using Puck's action plane damage criterion to predict the crack initiation and orientation [27]. The SEF known as the "risk of fracture" on the action plane is calculated for different angles using the material strength properties. In addition, the SEF can be differentiated for tensile and compressive normal stresses on the action plane as follows:

$$SEF(\theta)=\sqrt{\left(\frac{\tau_{nt}}{R^A_{\perp\perp}}\right)^2+\left(\frac{\tau_{n1}}{R^A_{\perp\parallel}}\right)^2+\left(\frac{p^{(-)}_{\perp\psi}}{R^A_{\perp\psi}}\sigma_n\right)^2}+\frac{p^{(-)}_{\perp\psi}}{R^A_{\perp\psi}}\sigma_n \quad for \;\; \sigma_n<0$$
$$SEF(\theta)=\sqrt{\left(\frac{1}{R^{(+)}_{\perp}}-\frac{p^{(+)}_{\perp\psi}}{R^A_{\perp\psi}}\right)^2\sigma_n^2+\left(\frac{\tau_{nt}}{R^A_{\perp\parallel}}\right)^2+\left(\frac{\tau_{n1}}{R_{\perp\parallel}}\right)^2}+\frac{p^{(+)}_{\perp\psi}}{R^A_{\perp\psi}}\sigma_n \quad for \;\; \sigma_n\geq 0 \tag{1}$$

where, σ_n is the normal stress, τ_{n1} stands for the transverse/longitudinal shear stress, and τ_{nt} is the transverse/transverse shear stress on the action plane. The longitudinal and transverse directions of the UD segments are specified by $\parallel$ and $\perp$ subscripts. $R^A_{\perp\perp}$, $R^A_{\perp\parallel}$ and $R^A_{\perp\psi}$ are fracture resistances of the action plane. The basic strengths of the material are tagged with $R^{(+)}_{\perp}$ and $R_{\perp\parallel}$.The inclination parameters from experimentally obtained (σ_2,τ_{12}) fracture curves are indicated by $p^{(+)}_{\perp\psi}$ and $p^{(-)}_{\perp\psi}$ [27]. Based on Puck's criterion, the damage onset appears when the SEF=1 and afterward the action plane becomes the fracture plane with $\theta=\theta_f$.

The damage is considered as degradation of mechanical properties in the UD segment. Ladeveze continuous damage model [28] based on energy release rate is applied as damage evolution law. The energy release rate Y_{12} is defined as the fictitious damage force defined as derivative of the elastic energy of damaged material Ψ regarding to the shear damage parameter [26]:

$$Y_{12}=\sqrt{\sup_{\tau\leq t}(Z_{12})},\;\; Z_{12}=-\frac{\partial\Psi}{\partial d_{12}} \tag{2}$$

where, $\sup(Z_{12})$ means the supremum energy release rate over time span of *t*. The square root in the above relation states that the energy release rate is positive-definite and preserves the non-healing damage condition. The Y_{12} value is defined using intact material stiffness constants C^0_{ij} and averaged principal ε and shear γ strains over the UD segment as [26]:

$$Z_{12}=\frac{\partial d_2}{\partial d_{12}}\varepsilon_{22}(\varepsilon_{22}C^0_{22}(1-d_2)+\varepsilon_{11}C^0_{12}+\varepsilon_{33}C^0_{23})+\frac{1}{2}(G^0_{12}\gamma^2_{12}+G^0_{23}\gamma^2_{23}) \tag{3}$$

Murakami's second rank stiffness tensor is used for progressive stiffness degradation [29]:

Excerpt from ISBN 978-3-00-053387-7

$$C^d = \begin{pmatrix} C_{11}^0 & C_{12}^0(1-d_2) & C_{13}^0 & 0 & 0 & 0 \\ & C_{22}^0(1-d_2)^2 & C_{23}^0(1-d_2) & 0 & 0 & 0 \\ & & C_{33}^0 & 0 & 0 & 0 \\ & & & G_{23}^0\left(\frac{2(1-d_2)}{2-d_2}\right)^2 & 0 & 0 \\ & sym. & & & G_{13}^0 & 0 \\ & & & & & G_{12}^0\left(\frac{2(1-d_2)}{2-d_2}\right)^2 \end{pmatrix} \quad (4)$$

The relation (4) shows that there are two damage parameters in the stiffness tensor for transverse and shear degradation. These damage parameters are linked together due to symmetry of the stress tensor proposed by Zako in[30]:

$$d_2 = \frac{2(1-\sqrt{1-d_{12}})}{2-\sqrt{1-d_{12}}} \quad (5)$$

Here, it is supposed that d_{12} is the main damage parameter and afterward the transverse damage parameter d_2 can be easily obtained from relation (5) [26]. Finally, Zinoviev's type [31] damage evolution law proposed by Ivanov et al. [26, 32] is implemented to incorporate the damage energy onset Y_{12}^0 and evolution Y_{12} with the main damage parameter as:

$$d_{12} = 1-\frac{Y_{12}^i}{Y_{12}}, \qquad Y_{12}^i = \sqrt{\varepsilon_{22}(\varepsilon_{22}C_{22}^0 + \varepsilon_{11}C_{12}^0 + \varepsilon_{33}C_{23}^0) + \frac{1}{2}(G_{12}^0\gamma_{12}^2 + G_{23}^0\gamma_{23}^2)} \quad (6)$$

The relation (6) states that the crack inside the UD segment propagates when the energy for damage evolution is greater than the damage onset energy i.e. $Y_{12} \geq Y_{12}^0$. To obtain the damage parameters, using relation (3), (5) and (6) an iterative numerical procedure based on Newton-Raphson's method is used [26]. The intra-yarn damage model described in this section as well as the matrix damage model in [24] are implemented in a FORTRAN subroutine for damage simulation of textile composites. The user defined material subroutine (UMAT) updates the material properties of the yarns and matrix according to the amount of damage accumulated during the FE analysis in ABAQUS.

4. RESULTS AND DISCUSSION

4.1. Warp/weft loading

The stress-strain curve in damage simulation of the multi-layer 2D plain weave composite is shown in Figure 3 for different mesh configurations. The pattern of shear and transverse damage parameters in the yarns is shown as well. As it's shown, there is a good agreement between the mesh superposition and experimental results in damage analysis of the multi-layer 2D plain weave composite in warp/weft loading. The FE results for all mesh configurations are overlapping that shows the mesh insensitivity of the numerical approach. The linear and non-linear material behaviour is well predicted using the applied damage algorithm in the UMAT script. There is a linear behaviour in stress-strain curve before crack initiation (around 0.20% of loading strain) after which the non-linearity in material starts due to progressive degradation of the mechanical properties. The damage initiation strain (%), first and second damage thresholds (%) are reported as 0.15±0.04, 0.26±0.04 and 0.43±0.06 in [19-20] based on acoustic emission measurements that coincide with the numerical simulations. The Young's modulus is predicted almost exact in the FE simulations with 26.5 GPa while it's 26±1.5 GPa in the experiments. The ultimate strength of the fabric is over predicted in the FE results for all mesh configurations with around 9.5% deviation from the experiment. From 0.2% to 1.2% the density of the transverse intra-yarn cracks increases. Then the transverse cracks span the yarn width and lead

Excerpt from ISBN 978-3-00-053387-7

to the second phase of damage in textile composites known as local delamination between the fibre bundles and matrix. The delamination growth is not captured in the mesh superposition method during damage simulation. This is due to the fact that in the MSP method the yarns are constrained with displacement equations and the interaction between the yarns and matrix to model the delamination is not considered.

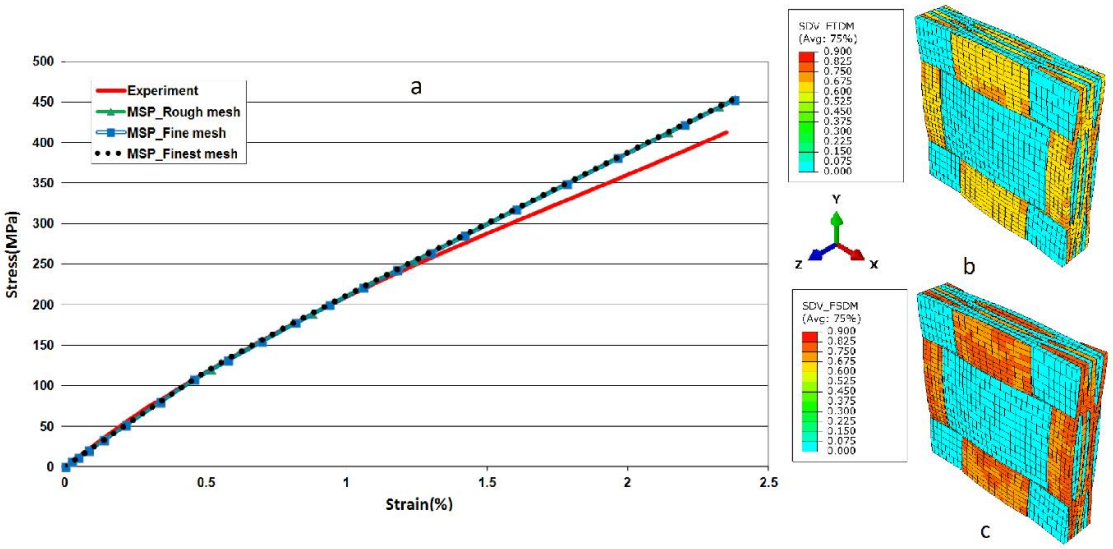

Figure 3. Damage modelling of a multi-layer 2D plain weave composite in warp/weft loading from mesh superposition (MSP) with different mesh configurations: (a) stress-strain curve, calculations and experiment [19-20]; (b) shear (d12) and (c) transverse (d2) damage parameters in the yarns.

4.2. Shear loading

In this part, the damage simulation of the multi-layer 2D plain weave composite during shear loading is validated with the experimental results. The ±45° specimens were loaded during standard tensile tests to emulate the shear behaviour of the fabric [19-20]. In FE analysis complex displacements are applied to the faces of the multi-layered meso- unit cell. As it's shown in Figure 4a, there is a remarkable compatibility between the experimental and numerical results. Here, the numerical results are reported up to 2.5% of shear strain but the experimental results reach to around 10% at the failure point. The stress-strain curve overlaps with the experimental results in the linear region up to 0.20% of shear strain. The shear modulus is calculated precisely in the MSP method with the amount of 12.6 GPa while *G* modulus is 12.20±0.40 in the experiment. From 0.25% to 0.75% of shear strain the numerical simulations over-predict the shear stresses that can be attributed to fibre bundle alignment along the 45° and contribution of contact stresses to avoid the interpenetrations in the MSP method. It should be noted that the meso-FE unit cell has an ideal geometrical configuration in which the nesting of the layers has not been considered in the simulations. As a result, a portion of the transferred load during the FE modelling disappears in yarn adjustment. After fibre bundle alignment in 45° that coincides with 1% of shear strain, there is a good agreement between the MSP and experimental results. Figure 4b shows the incrementally damage evolution in the yarns based on Puck's damage criterion.

Excerpt from ISBN 978-3-00-053387-7

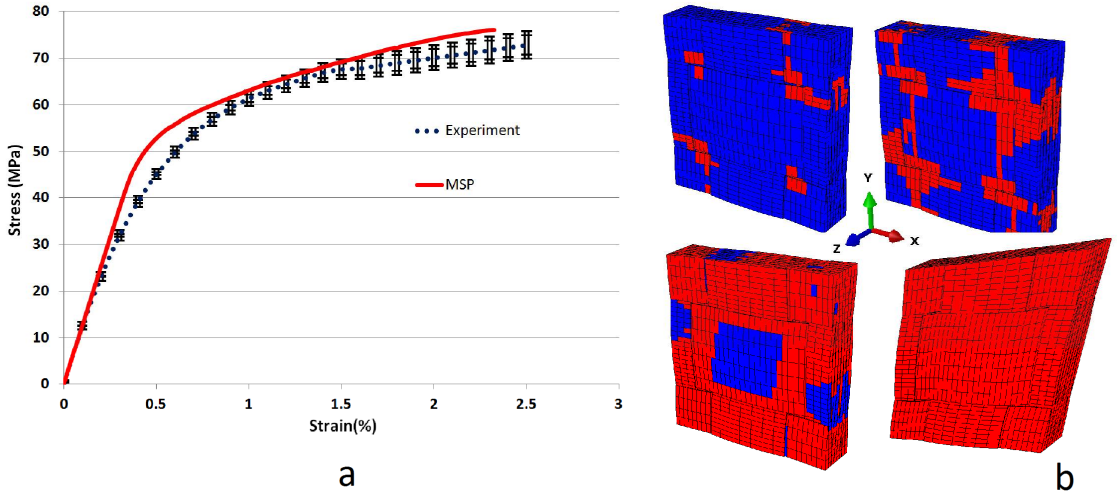

Figure 4. Damage modelling of a multi-layer 2D plain weave composite in bias loading from mesh superposition (MSP) with different mesh configurations: (a) stress-strain curve, calculations and experiment [19-20]; (b) damage evolution parameter (Puck's criterion) in the yarns, different loading stages.

5. CONCLUSIONS

The feasibility of usage of MSP method in meso-FE damage modelling of textile composites is confirmed after comparison with the experimental data for a glass/epoxy woven laminate. To summarize, the MSP method opens ways to meso-FE modelling of textile composites which involves a fast and accurate geometric representation without limitations for the numerical analysis of textile structures in linear/non-linear region. However, the delamination modeling is not included in the MSP method in this research that can be a subject for future work.

Acknowledgments

The work leading to this publication has been partially funded by the M3Strength ICON project, which fits in the MacroModelMat (M3) research program funded by SIM (Strategic Initiative Materials in Flanders) and IWT (Flemish government agency for Innovation by Science and Technology).

References

[1] Tabatabaei SA, Lomov SV, Verpoest I. Assessment of embedded element technique in meso-FE modelling of fibre reinforced composites. *Composite Structures*. 2014;107:436-46.
[2] Tabatabaei SA, Lomov SV. Eliminating the volume redundancy of embedded elements and yarn interpenetrations in meso-finite element modelling of textile composites. *Computers & Structures*. 2015;152:142-54.
[3] Tabatabaei SA, Swolfs Y, Wu H, Lomov SV. Full-field strain measurements and meso-FE modelling of hybrid carbon/self-reinforced polypropylene. *Composite Structures*. 2015;132:864-73.
[4] Abaqus 6.11 doumentation.
[5] Ortiz M, Leroy Y, Needleman A. A finite element method for localized failure analysis. *Computer Methods in Applied Mechanics and Engineering*. 1987;61:189-214.
[6] Soh A-K, Wanji C. Finite element formulations of strain gradient theory for microstructures and the C0–1 patch test. *International Journal for Numerical Methods in Engineering*. 2004;61:433-54.
[7] Paz M, Leigh W. Static Condensation and Substructuring. Integrated Matrix Analysis of Structures: *Theory and Computation*. Boston, MA: Springer US; 2001. p. 239-60.
[8] Belytschko T, Fish J, Engelmann BE. A finite element with embedded localization zones. Computer Methods in Applied Mechanics and Engineering. 1988;70:59-89.
[9] Fish J, Belytschko T. Elements with embedded localization zones for large deformation problems. In: Noor AK, Dwoyer DL, editors. *Computational Structural Mechanics & Fluid Dynamics*. Oxford: Pergamon; 1988. p. 247-56.

Excerpt from ISBN 978-3-00-053387-7

[10] Fish J. The s-version of the finite element method. Computers & Structures. 1992;43:539-47.
[11] Zako M, Kurashiki T, Imura M. A multi-scale analysis for structural design of fibrous Composites –M3 method. *15th International Conference on Composite Materials*. Durban, South Africa2005.
[12] Zako M, V.Lomov S, Verpost I. FE and damage modelings in textile composites. *Finite element modelling of textiles and textile composites*. St-Petersburg, 2007.
[13] Kurashiki T, Zako M, Nakai H, Imura M, Hirosawa S. Damage development of woven composites based on multi-scale analysis. *16th International Conference On Composite Materials* Kyoto, Japan, 2007.
[14] Honda S, Zako M, Kurashiki T, Nakai H, Lomov S, Verpoest I. A proposal of stress/strain analytical procedure of textile composites with stitch by M3 method. *13th European Conference on Composite Materials (ECCM-13)*. Stockholm, Sweden2008.
[15] Ohyama D, Kurashiki T, Watanabe Y, Fujita Y, Zako M. Estimation of mechanical behavior of braided composites based on superposition method. *18th International Conference On Composite Materials*. Jeju Island, South Korea2011.
[16] Jiang WG, Hallett S, Wisnom M. Development of Domain Superposition Technique for the Modelling of Woven Fabric Composites. *Mechanical Response of Composites*. 2008;10:281-91.
[17] Iarve EV, Mollenhauer DH, Zhou EG, Breitzman T, Whitney TJ. Independent mesh method-based prediction of local and volume average fields in textile composites. Composites Part A: *Applied Science and Manufacturing*. 2009;40:1880-90.
[18] Iarve EV, Mollenhauer DH, Zhou E, Whitney TJ. Stress analysis in complex fiber architecture composites: independent mesh method. *Finite element modelling of textiles and textile composites*. St-Petersburg.
[19] Lomov SV, Bogdanovich AE, Ivanov DS, Mungalov D, Karahan M, Verpoest I. A comparative study of tensile properties of non-crimp 3D orthogonal weave and multi-layer plain weave E-glass composites. Part 1: Materials, methods and principal results. *Composites Part A: Applied Science and Manufacturing*. 2009;40:1134-43.
[20] Ivanov DS, Lomov SV, Bogdanovich AE, Karahan M, Verpoest I. A comparative study of tensile properties of non-crimp 3D orthogonal weave and multi-layer plain weave E-glass composites. Part 2: Comprehensive experimental results. *Composites Part A: Applied Science and Manufacturing*. 2009;40:1144-57.
[21] Verpoest I, Lomov SV. Virtual textile composites software WiseTex: Integration with micro-mechanical, permeability and structural analysis. *Composites Science and Technology*. 2005;65:2563-74.
[22] Lomov SV, Verpoest I, Cichosz J, Hahn C, Ivanov DS, Verleye B. Meso-level textile composites simulations: Open data exchange and scripting. *Journal of Composite Materials*. 2013.
[23] Lomov SV, Bogdanovich AE, Ivanov DS, Hamad K, al. e. Finite element modelling of progressive damage in non-crimpt 3D orthogonal weave and plain weave E-glass composites. *2ND World Conference on 3D Fabrics*. Greenville2009.
[24] Melro AR, Camanho PP, Andrade Pires FM, Pinho ST. Micromechanical analysis of polymer composites reinforced by unidirectional fibres: Part I – Constitutive modelling. *International Journal of Solids and Structures*. 2013;50:1897-905.
[25] Talreja R. A continuum mechanics characterization of damage in composite materials. Proceedings of the Royal Society of London A: *Mathematical, Physical and Engineering Sciences*: The Royal Society; 1985. p. 195-216.
[26] Ivanov DS, Lomov SV. 2 - Modelling the structure and behaviour of 2D and 3D woven composites used in aerospace applications A2 - Irving, P.E. In: Soutis C, editor. Polymer Composites in the Aerospace Industry: *Woodhead Publishing*; 2015. p. 21-52.
[27] Puck A, Kopp J, Knops M. Guidelines for the determination of the parameters in Puck's action plane strength criterion. *Composites Science and Technology*. 2002;62:371-8.
[28] Ladèveze P, Lubineau G. An enhanced mesomodel for laminates based on micromechanics. *Composites Science and Technology*. 2002;62:533-41.
[29] Murakami S. Mechanical Modeling of Material Damage. Journal of Applied Mechanics. 1988;55:280-6.
[30] Zako M, Uetsuji Y, Kurashiki T. Finite element analysis of damaged woven fabric composite materials. *Composites Science and Technology*. 2003;63:507-16.
[31] Zinoviev PA, Grigoriev SV, Lebedeva OV, Tairova LP. The strength of multilayered composites under a plane-stress state. *Composites Science and Technology*. 1998;58:1209-23.
[32] Ivanov DS, Baudry F, Van Den Broucke B, Lomov SV, Xie H, Verpoest I. Failure analysis of triaxial braided composite. *Composites Science and Technology*. 2009;69:1372-80.

Excerpt from ISBN 978-3-00-053387-7